

## ANTI-PLANE SHEAR CRACKS IN IDEALLY PLASTIC CRYSTALS

JAMES R. RICE and RUZICA NIKOLIC

Division of Applied Sciences, Harvard University, Cambridge, MA 02138, U.S.A.

(Received 4 October 1984; in revised form 13 February 1985)

### ABSTRACT

CRACKS in ductile single crystals are analyzed here for geometries and orientations such that two-dimensional states of anti-plane shear constitute possible deformation fields. The crystals are modelled as ideally plastic and yield according to critical resolved shear stresses on their slip systems. Restrictions on the asymptotic forms of stress and deformation fields at crack tips are established for anti-plane loading of stationary and quasistatically growing cracks, and solutions are presented for several specific orientations in f.c.c. and b.c.c. crystals. The asymptotic solutions are complemented by complete elastic-plastic solutions for stationary and growing cracks under small scale yielding, based on previous work by RICE (1967, 1984) and FREUND (1979). Remarkably, the plastic zone at a stationary crack tip collapses into discrete planes of displacement and stress discontinuity emanating from the tip; plastic flow consists of concentrated shear on the displacement discontinuities. For the growing crack these same planes, if not coincident with the crack plane, constitute collapsed plastic zones in which velocity and plastic strain discontinuities occur, but across which the stresses and anti-plane displacement are fully continuous. The planes of discontinuity are in several cases coincident with crystal slip planes but it is shown that this need not be the case, e.g., for orientations in which anti-plane yielding occurs by multi-slip, or for special orientations in which the crack tip and the discontinuity planes are perpendicular to the activated slip plane.

### 1. INTRODUCTION

THIS article analyzes stress and deformation fields around crack tips for both stationary and growing cracks in ductile single crystals subjected to anti-plane shear and oriented so that two-dimensional anti-plane strain is a possible deformation state. The material is considered as elastic-perfectly plastic and both asymptotic and complete analyses are carried out. The plastic yield condition in single crystals is of the type that the shear stress on each possible slip system is bounded by the strength for that system. Thus the response is anisotropic, but with a flow rule of associated type. For the complete solutions developed, small scale yielding is considered, i.e. it is assumed that the plastic zone dimensions are small in comparison with the crack length.

Previous work on this problem has been presented for the stationary crack case by RICE (1967, 1984). He devised a solution method for an edge crack or V-notch in a general anisotropic ideally plastic half space under anti-plane conditions, based on the well known "hodograph" type transformation. He also presented some specific results for cracks under small scale yielding in solids with yield surfaces consisting (like those in crystals) of straight-line segments in a two-dimensional stress space whose coordinates

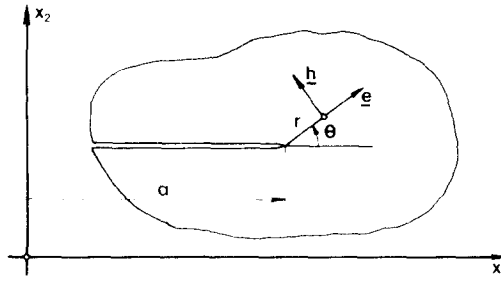


FIG. 1. Coordinate systems and notations used:  $x_1, x_2, x_3$ —Cartesian system;  $r, \theta$ —polar coordinates centered at crack tip;  $\mathbf{e}, \mathbf{h}$ —unit vectors in radial and angular directions, respectively;  $a$ —crack length.

are the anti-plane shear stress components. For yield surfaces of the type mentioned, it was shown that the plastic zone collapsed to planes of displacement discontinuity emanating from the notch tip. We adopt the Rice solution method later in the paper to present results for small scale yielding at stationary crack tips in some specific crystal geometries. We also present results which are new in character on the form of the near tip stress and deformation fields for quasistatic growth in ideally plastic crystals. These results are primarily asymptotic in character and are developed by first extending, and specializing to the single crystal context, asymptotic results by RICE (1982) on quasistatic crack growth in ideally plastic solids of arbitrary anisotropy.

Coordinate systems adopted for this analysis are shown in Fig. 1. The fixed Cartesian system  $x_1, x_2, x_3$  is chosen so that  $x_3$  is parallel to the crack front and  $x_1$  is pointing in the direction of crack growth. Polar coordinates  $r, \theta$  lie in the  $x_1, x_2$  plane, have origin at the possibly moving crack tip and have the associated unit vectors  $\mathbf{e}$  and  $\mathbf{h}$  in the radial and angular directions, respectively. It is evident that

$$\partial r / \partial x_\alpha = e_\alpha, \quad \partial \theta / \partial x_\alpha = h_\alpha / r, \quad (1)$$

where

$$e_1 = h_2 = \cos \theta, \quad e_2 = -h_1 = \sin \theta, \quad e_3 = h_3 = 0. \quad (2)$$

Greek indices have values 1, 2 and follow the summation convention. Exception is made for  $\theta$ ; indices  $r$  and  $\theta$  always denote components relative to the polar coordinates. The crystal orientations and loadings considered are such that the only non-vanishing stresses are  $\sigma_{13} = \sigma_{31} = \tau_1$  and  $\sigma_{23} = \sigma_{32} = \tau_2$ .

## 2. GOVERNING EQUATIONS

### *Equilibrium*

The equilibrium equation for anti-plane shear is

$$\tau_{\alpha,\alpha} + f = 0, \quad (3)$$

where  $f$  is the body force, or, in polar coordinates,

$$(\partial \tau_\alpha / \partial \theta) h_\alpha + r(\partial \tau_\alpha / \partial r) e_\alpha + r f = 0. \quad (4)$$

For the asymptotic analysis of the stress field around the crack tip we assume that, because of boundedness of stress,  $r(\partial\tau_\alpha/\partial r) \rightarrow 0$  as  $r \rightarrow 0$  so the second and third terms in (4) vanish as  $r \rightarrow 0$ . Hence, in that limit the equilibrium equation requires that

$$h_\alpha \tau'_\alpha = 0, \tag{5}$$

where  $\tau'_\alpha = \lim_{r \rightarrow 0} [\partial\tau_\alpha(r, \theta, t)/\partial\theta]$ . Equation (5) can by use of (2) be written as

$$e_2 \tau'_1 = e_1 \tau'_2 \tag{6}$$

or, in polar coordinates as

$$\tau_r + \tau'_\theta = 0. \tag{7}$$

*Yield condition*

A plastic yield condition is in general presumed to take a form  $f(\sigma) = 0$  where  $\sigma$  is the stress tensor. This is the equation of a curve in the two-dimensional  $\sigma$  space with coordinates denoted by  $\tau_1, \tau_2$ ; we refer to this curve as the yield surface. However, in single crystals as they are modelled conventionally, the yield surface consists of straight-line segments. This is because in crystals slip can occur only on certain planes and in certain directions (e.g.  $\{111\}$  planes and  $\langle 110 \rangle$  directions in face-centered cubic crystals), i.e. on particular slip systems. Thus the allowable states of stress are given by

$$\tau^{(k)} \equiv n_1^{(k)} \sigma_{ij} s_j^{(k)} = n_3^{(k)} \tau_\alpha s_\alpha^{(k)} + n_\alpha^{(k)} \tau_\alpha s_3^{(k)} \leq \tau_0^{(k)} \tag{8}$$

( $i, j = 1, 2, 3; \alpha = 1, 2$ ),

where  $\tau^{(k)}$  is the resolved shear stress on the  $k$ th slip systems,  $n_3^{(k)}, n_\alpha^{(k)}$  are the components of the unit normal of the slip plane,  $s_3^{(k)}, s_\alpha^{(k)}$  are the components of the unit vector in the slip direction, and  $\tau_0^{(k)}$  is the yield strength for the  $k$ th slip system. Thus for each slip system in a given crystal we will have a line in  $\tau$  space whose equation is of the form  $m_1^{(k)} \tau_1 + m_2^{(k)} \tau_2 = \tau_0^{(k)}$ . The yield surface is the inner envelope of this set of lines as shown in Fig. 2, and  $\mathbf{m}^{(k)} [= (m_1^{(k)}, m_2^{(k)})]$  is a vector in the outer normal direction to a given line.

*Stress-strain relations*

The rate of deformation is given by

$$\dot{\gamma}_\alpha \equiv \dot{\epsilon}_{,\alpha} = \dot{\gamma}_\alpha^e + \dot{\gamma}_\alpha^p, \tag{9}$$

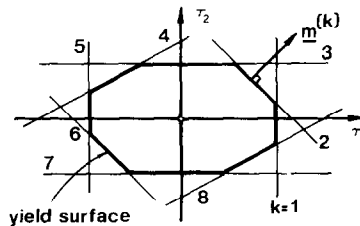


FIG. 2. Yield surface for a single crystal as the inner envelope of the set of lines corresponding to critical stressing of the separate slip systems.

where  $u$  is the displacement in the  $x_3$  direction. The elastic deformation is

$$\gamma_\alpha^e = c_{\alpha\beta} \tau_\beta, \quad (10)$$

where  $c_{\alpha\beta}$  is  $2 \times 2$  matrix of elastic compliances, and the plastic strain rate is

$$\dot{\gamma}_\alpha^p = \sum_k \dot{\gamma}^{(k)} (n_3^{(k)} s_\alpha^{(k)} + n_\alpha^{(k)} s_3^{(k)}) = \sum_k \dot{\gamma}^{(k)} m_\alpha^{(k)}, \quad (11)$$

where  $\dot{\gamma}^{(k)} \geq 0$  and  $\sum_k$  denotes the summation over all active slips systems (with index  $k$ ).  $\dot{\gamma}^{(k)} > 0$  only if the equality holds in (8). Sometimes, several symmetrically oriented slip systems must be active simultaneously to produce (only) anti-plane strain. Hence a single yield surface segment of normal  $\mathbf{m}$  may correspond to more than one active slip system, and a vertex where two segments join may correspond to more than two active systems. The flow rule is of associated type and this corresponds to normality of  $\dot{\gamma}_\alpha^p$  to the yield surface in the  $\tau_\alpha$  plane (or to  $\dot{\gamma}_\alpha^p$  having the direction within the fan defined by limiting normals at a vertex). For elastically isotropic crystals as well as for some high-symmetry orientations of cubic crystals (10) can be written as

$$\gamma_\alpha^e = c_{\alpha\beta} \tau_\beta = (1/\mu) \tau_\alpha, \quad (12)$$

where  $\mu$  is the shear modulus.

### 3. STRESS AND STRAIN FIELDS IN DIFFERENT SECTORS AROUND THE CRACK TIP

In general, there will be zones of material that currently deform only elastically and zones that currently respond plastically. The former zones may be either of a type that has previously yielded but now responds elastically, or of a type that has always responded elastically. Thus, around the crack tip we will have some combinations of what we call "elastic sectors", i.e. regions of material that currently respond elastically, and "plastic sectors", i.e. regions of material that are currently plastically active. The full stress and strain fields around the crack tip will be obtained by assembling different types of sectors and satisfying certain continuity conditions across the lines that are boundaries between sectors.

#### *Elastic sectors*

Elastic sectors can either be of constant stress type,  $\tau'_\alpha = 0$ , or a more general type in which  $\tau'_\alpha \neq 0$ . Starting from the compatibility condition

$$\partial\gamma_1/\partial x_2 = \partial\gamma_2/\partial x_1 \quad (13)$$

we consider first a sector which has always responded elastically or which, if previously yielded, is such that the  $\gamma_\alpha^p$  are finite and do not vary with  $\theta$  as  $r \rightarrow 0$ . This is the type of elastic sector found at a stationary crack tip. In such a case it suffices for asymptotic analysis to use the elastic constitutive relation (10). Using  $r(\partial\tau_\alpha/\partial r) \rightarrow 0$  as  $r \rightarrow 0$  we

obtain from (13) and (1) that

$$c_{1\alpha}\tau'_\alpha h_2 = c_{2\alpha}\tau'_\alpha h_1, \quad (14)$$

or by making use of (2)

$$c_{1\alpha}\tau'_\alpha e_1 + c_{2\alpha}\tau'_\alpha e_2 = e_\beta c_{\beta\alpha}\tau'_\alpha = 0. \quad (15)$$

Taking into account the equilibrium condition (6) from which we can write  $\tau'_1 = (e_1/e_2)\tau'_2$ , this becomes

$$e_\beta c_{\beta 1}(e_1/e_2)\tau'_2 + e_\beta c_{\beta 2}\tau'_2 = e_\beta c_{\beta\alpha}e_\alpha\tau'_2/e_2 \equiv c_{rr}\tau'_2/e_2 = 0, \quad (16)$$

where  $c_{rr} \equiv e_\alpha c_{\alpha\beta}e_\beta$ . Since  $c_{rr} \neq 0$  it follows that

$$\tau_1 = \text{constant} \quad \text{and} \quad \tau_2 = \text{constant} \quad (17)$$

in the sense that in the limit  $r \rightarrow 0$  the stress components are independent of  $\theta$  (or "constant") in such an elastic sector.

A more general type of elastic sector in which  $\tau'_\alpha \neq 0$  is possible for the growing crack case. This arises in sectors of material that currently respond elastically but have previously yielded in the crack tip singularity. We write  $\tau_\alpha = \tau_\alpha(r, \theta, t)$  and then we have for the stress rate

$$\dot{\tau}_\alpha = (\partial\tau_\alpha/\partial r)\dot{r} + (\partial\tau_\alpha/\partial\theta)\dot{\theta} + (\partial\tau_\alpha/\partial t) = (\partial\tau_\alpha/\partial r)(-e_1\dot{a}) + (\partial\tau_\alpha/\partial\theta)(e_2\dot{a}/r) + (\partial\tau_\alpha/\partial t), \quad (18)$$

where use is made of  $\dot{r} = -e_1\dot{a}$  and  $\dot{\theta} = e_2\dot{a}/r$  when we follow a material point. Since  $r(\partial\tau_\alpha/\partial r) \rightarrow 0$  as  $r \rightarrow 0$  and we may assume  $r(\partial\tau_\alpha/\partial t) \rightarrow 0$ , it follows from (18) that

$$r\dot{\tau}_\alpha \rightarrow \tau'_\alpha e_2\dot{a}. \quad (19)$$

This means that the stress rates, and hence elastic strain rates, are singular as  $\dot{a}/r$  in sectors around the crack tip in which  $\tau'_\alpha \neq 0$ . If we make use of (10) and (19) we can write

$$\dot{\gamma}_\alpha = c_{\alpha\beta}\dot{\tau}_\beta \rightarrow c_{\alpha\beta}\tau'_\beta e_2\dot{a}/r. \quad (20)$$

Now we make use of compatibility condition

$$\dot{\gamma}_{1,2} = \dot{\gamma}_{2,1} \quad (21)$$

and we write this with the use of (20) and (1) as

$$(c_{1\beta}\tau'_\beta e_2)(-\dot{a}e_2/r^2) + (c_{1\beta})(\tau'_\beta e_2)'(\dot{a}h_2/r^2) = (-c_{2\beta}\tau'_\beta e_2)(\dot{a}e_1/r^2) + (c_{2\beta})(\tau'_\beta e_2)'(\dot{a}h_1/r^2). \quad (22)$$

Now using (2) and knowing that  $c_{r\beta} \equiv e_\alpha c_{\alpha\beta}$  and  $c'_{r\beta} = h_\alpha c_{\alpha\beta} \equiv c_{\theta\beta}$ , we obtain from (22)

$$c_{r\beta}(\tau'_\beta e_2)' + c_{\theta\beta}(\tau'_\beta e_2) = [c_{r\beta}(\tau'_\beta e_2)]' = 0. \quad (23)$$

Hence

$$c_{r\beta}\tau'_\beta e_2 = \text{constant}, \quad (24)$$

which we can rewrite using  $\tau'_1 = (e_1/e_2)\tau'_2$  from (6) as

$$(e_\alpha c_{\alpha\beta}e_\beta)\tau'_2 \equiv c_{rr}\tau'_2 = \text{constant}. \quad (25)$$

Thus, in elastic sectors of the type considered

$$\begin{aligned}\tau_2 &= A - \hat{B} \int [c_{rr}(\theta)]^{-1} d\theta, \\ \tau_1 &= C - \hat{B} \int (\sin \theta)^{-1} \cos \theta [c_{rr}(\theta)]^{-1} d\theta,\end{aligned}\tag{26}$$

where  $A$  and  $\hat{B}$  are constants. This includes the constant stress sector as a special case,  $\hat{B} = 0$ . For the case of an isotropic material,  $c_{rr} = 1/\mu$  independently of  $\theta$ , the expressions for stresses (26) reduce to the known relations (RICE 1982)

$$\tau_2 = A - B\theta, \quad \tau_1 = C - B \ln(\sin \theta).\tag{27}$$

Since  $\partial \dot{u}/\partial r = e_z \dot{\gamma}_z$ , we have from (20) and the steps from (24)–(26) that the velocity field in such elastic sectors satisfies

$$\partial \dot{u}/\partial r \rightarrow e_\alpha c_{\alpha\beta} \tau'_\beta e_2 \dot{a}/r = c_{rr} \tau'_2 \dot{a}/r = -\hat{B} \dot{a}/r.\tag{28}$$

Thus, the velocity field is singular in the form  $\dot{u} \rightarrow \hat{B} \dot{a} \ln(L/r)$ ,  $L$  having length dimensions, in such elastic sectors at a growing crack tip.

### Plastic sectors

Plastic sectors are regions of material around the crack tip that are currently stressed to yield and deform plastically. Their discussion here applies also to the special case of sectors that are instantaneously stressed to yield but do not further strain (as in stationary crack solutions by RICE (1967, 1984)), or do so only elastically by unloading. See section 3 for further discussion. Such sectors for general anisotropic solids can be of constant stress type or of variable stresses (centered fan sectors, RICE (1982)). For single crystal yield surfaces as given in Fig. 2 it is now shown that we shall have only sectors of the first type, i.e. with constant stresses. It is evident that in any sector that is stressed to yield, a relation of type  $m_1 \tau_1 + m_2 \tau_2 = \tau_0 = \text{constant}$  is satisfied. This refers to a straight-line segment of the yield surface whose outer normal is  $\mathbf{m}$ . If the stress state in a sector lies simultaneously on two such non-collinear line segments, i.e. if the state is at a vertex, then  $\tau_1$  and  $\tau_2$  are necessarily fixed and the sector is of constant stress type (and not only as  $r \rightarrow 0$ ). Hence, we now consider the case of stresses on a single line segment, in which case

$$m_1 \tau'_1 + m_2 \tau'_2 = 0\tag{29}$$

within the segment. When combined with the equilibrium equation in asymptotic form  $e_2 \tau'_1 = e_1 \tau'_2$  there results

$$(m_1 e_1 + m_2 e_2)(\tau'_2/e_2) = 0.\tag{30}$$

Hence, everywhere except possibly along the single ray from the crack tip for which  $\mathbf{e}$  is perpendicular to  $\mathbf{m}$ , i.e.  $\mathbf{m} \cdot \mathbf{e} = 0$ , the result (29) implies that  $\tau'_1 = \tau'_2 = 0$  and hence that the sector is of constant stress type. It will be seen shortly that the special ray mentioned is, in fact, one along which stress and displacement discontinuities are permissible for a stationary crack, and velocity discontinuities for a growing crack. It is a ray to which the associated plastic strain rate is perpendicular, by (11).

*Assembling sectors: stationary crack*

For the case of a stationary crack we obtained the result that possible sectors around the crack tip are either elastic or plastic sectors of constant stress type. Therefore, to assemble such sectors in the full field around the crack tip, the existence of discontinuities is necessary if the crack surface boundary conditions  $\tau_2 = 0$  are to be satisfied while transmitting shear  $\tau_2 \neq 0$  ahead of the crack. As suggested by the equilibrium equation written in the form of (7), we have the requirement that  $\tau_\theta$  must be continuous, and thus only  $\tau_r$  is discontinuous across the line between two different constant stress sectors. This suggests that  $\gamma_r$  may be discontinuous at sector boundaries, and this is what occurs in solutions presented by RICE (1967, 1984). Hence we consider discontinuities along which possibly

$$\partial \llbracket u \rrbracket / \partial r \neq 0, \quad \llbracket u \rrbracket = u^- - u^+, \quad (31)$$

where  $u^+$  and  $u^-$  are the values of displacement just ahead of, and just behind a line of discontinuity, respectively, which implies that  $u$  is discontinuous across that line. This displacement discontinuity, when regarded as a concentrated plastic shear of type  $\gamma_b^p$ , is consistent with the flow rule (11) *only* if the discontinuity is such that the vector  $\mathbf{h}$  along it is a direction of plastic shear  $\gamma^p$  allowed by the flow rule (11). Thus the stress state on at least one side of such a purported discontinuity must be at yield and such that the yield surface outer normal  $\mathbf{m}$  of Fig. 2 (or some positive linear combination of two  $\mathbf{m}$  vectors at a vertex) is in the direction of  $\mathbf{h}$ .

Let us examine the case, arising in specific solutions, that both sides of the discontinuity are stressed to yield in a manner consistent with concentrated plastic shear along the discontinuity. Then stress states on both sides of the discontinuity lie along a yield surface segment with normal  $\mathbf{m}$  and, analogously to (29)

$$m_1 \llbracket \tau_1 \rrbracket + m_2 \llbracket \tau_2 \rrbracket = 0. \quad (32)$$

Since from equilibrium  $\tau_\theta = h_x \tau_x$  is continuous, we also have

$$h_1 \llbracket \tau_1 \rrbracket + h_2 \llbracket \tau_2 \rrbracket = 0 \quad (\text{or } e_2 \llbracket \tau_1 \rrbracket = e_1 \llbracket \tau_2 \rrbracket), \quad (33)$$

and the last two conditions can be satisfied simultaneously only if, analogously to (30),

$$(m_1 e_1 + m_2 e_2) \llbracket \tau_2 \rrbracket / e_2 = 0. \quad (34)$$

Hence such a discontinuity (for which  $\llbracket \tau_1 \rrbracket, \llbracket \tau_2 \rrbracket \neq 0$ ) is possible only along a ray from the tip for which  $\mathbf{e}$  is perpendicular to  $\mathbf{m}$ , because then  $m_1 e_1 + m_2 e_2 = 0$ .

That is, the sector boundaries are defined by rays of stress and displacement discontinuities for which  $\mathbf{h}$  of the ray has the direction of  $\mathbf{m}$ . As revealed in the solutions by RICE (1967, 1984), for the stationary crack under loadings inducing  $\tau_2 > 0$  ahead of the crack, the field at the tip consists of an array of constant stress sectors at yield. These sectors have a stress state corresponding to the vertices of the yield surface (or, along the crack faces, to the points on the  $\tau_1$  axis where  $\tau_2 = 0$ ), and the stress state jumps discontinuously from vertex to vertex along the ray for which  $\mathbf{h}$  has the direction  $\mathbf{m}$  of the normal to the yield surface segment joining the vertices (i.e. along the ray in the  $x_1, x_2$  plane which is parallel to the considered yield surface segment in the  $\tau_1, \tau_2$  plane).

*Assembling sectors: growing crack*

For the case of a growing crack, possible sectors around the crack tip are elastic sectors of possibly variable stresses and plastic sectors of necessarily constant stress type. Following DRUGAN and RICE (1984) where a complete discussion on discontinuities across a quasistatically moving surface is given, we consider now what kinds of discontinuities may emerge on the ray which is the boundary between the two types of sectors mentioned. A ray of displacement discontinuity cannot move perpendicular to itself so we have

$$\dot{a}h_1 \llbracket u \rrbracket = 0, \tag{35}$$

where  $\dot{a}h_1$  is its velocity normal to itself; here  $\mathbf{h}$  is the unit vector perpendicular to the ray of discontinuity. So we have that the displacement is continuous everywhere except possibly on the crack plane itself. Note that if  $\llbracket u \rrbracket = 0$ , then  $e_x \llbracket \gamma_x \rrbracket = 0$ . Also from equilibrium

$$h_x \llbracket \tau_x \rrbracket = 0 \tag{36}$$

(as in equation (33)). Now we make use of the principle of maximum plastic work (identically satisfied by the constitutive description of (8) and (11)) which in our case can be written as

$$(\tau_x - \tau_x^0) \dot{\gamma}_x^p \geq 0, \tag{37}$$

where  $\tau_x$  is the actual stress state and  $\tau_x^0$  is any other stress state with stresses at or below yield. Following the DRUGAN and RICE (1984) procedure, if we take  $\tau_x^0 = \tau_x^+$  and integrate (37) across the ray of discontinuity we have

$$\int_+ \ (\tau_x - \tau_x^+) (d\gamma_x - d\gamma_x^e) \geq 0, \tag{38}$$

where  $+$  and  $-$  are the respective forward and rear sides of the discontinuity ray; values with superscript  $+$  are evaluated immediately before and those with superscript  $-$  immediately after the discontinuity. By the kinematic and equilibrium requirements above,  $(\tau_x - \tau_x^+) d\gamma_x$  vanishes identically in the integration, and hence with  $d\gamma_x^e = c_{\alpha\beta} d\tau_\beta$ ,

$$-\int_+ \ (\tau_x - \tau_x^+) c_{\alpha\beta} d(\tau_\beta - \tau_\beta^+) = -\frac{1}{2} \llbracket \tau_\alpha \rrbracket c_{\alpha\beta} \llbracket \tau_\beta \rrbracket \geq 0, \tag{39}$$

which proves that  $\llbracket \tau_\alpha \rrbracket = 0$  since  $c_{\alpha\beta}$  is positive definite. Thus we have a fully continuous stress field. The significance of this remark is that the only way that stress can vary from that of a (constant stress) plastic sector is if that sector is bordered by an elastic sector of type discussed in the first part of section 3.

As in general discussion by DRUGAN and RICE (1984), a velocity discontinuity at the interface is not prohibited, so long as it is consistent with the flow rule. Thus if the stress state at the discontinuity is such that the yield surface outer normal  $\mathbf{m}$  (or some positive linear combination of the two  $\mathbf{m}$ s at a vertex) is in the direction of  $\mathbf{h}$ , a velocity discontinuity  $\llbracket \dot{u} \rrbracket \neq 0$  is allowed.

Now we consider, using these general conclusions, the boundary between a plastic and elastic sector; Fig. 3. From the expression of (28) for  $\partial \dot{u} / \partial r$  in an elastic sector we

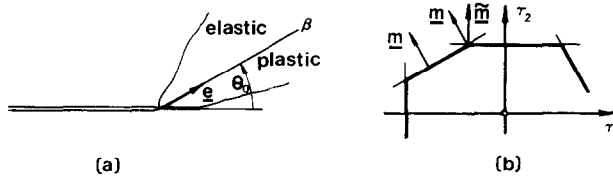


FIG. 3. (a) Detail of the stress field around the crack tip; plastic sector (sector with stresses at yield) and neighboring elastic sector with boundary  $\beta$  between them. (b) Corresponding detail of the yield surface.

can write

$$\mathbf{e} \cdot \dot{\boldsymbol{\gamma}} = -\hat{B}\dot{a}/r \quad (40)$$

and from equations (26) for  $\tau_1$  and  $\tau_2$ , that

$$\boldsymbol{\tau}' = -\mathbf{e}\hat{B}/e_2c_{rr}. \quad (41)$$

If the stress state in the plastic region is at yield on a segment with normal  $\mathbf{m}$ , then it is necessary that the unloading condition  $e_2\mathbf{m} \cdot \boldsymbol{\tau}' \leq 0$  be met as the elastic region is entered at  $\beta$  (the factor  $e_2$  caters to the sign of  $\theta$  at the discontinuity). We shall handle the possibility that the stress state is at a vertex, and hence also on a segment where the normal is  $\tilde{\mathbf{m}}$ , by appending results pertaining to  $\tilde{\mathbf{m}}$  in square brackets [...]; these are to be disregarded when the stress state is not at a vertex. Thus the unloading condition, using (41), is

$$\hat{B}\mathbf{m} \cdot \mathbf{e} \geq 0 \quad [\hat{B}\tilde{\mathbf{m}} \cdot \mathbf{e} \geq 0]. \quad (42)$$

In the plastic sector we have from the flow rule that

$$\dot{\boldsymbol{\gamma}} = \Lambda\mathbf{m} [ + \tilde{\Lambda}\tilde{\mathbf{m}} ], \quad (43)$$

where  $\Lambda \geq 0$  [and  $\tilde{\Lambda} \geq 0$ ] is a scalar.

We now enumerate two possibilities: that the interface at  $\beta$  either (i) is, or (ii) is not an interface of velocity continuity. Consider case (i) first. In that case  $\mathbf{e} \cdot \dot{\boldsymbol{\gamma}}$  must be continuous at the interface, and hence from (40) and (43)

$$-\hat{B}\dot{a}/r = \Lambda\mathbf{e} \cdot \mathbf{m} [ + \tilde{\Lambda}\mathbf{e} \cdot \tilde{\mathbf{m}} ]. \quad (44)$$

Multiplying through with  $\hat{B}$ ,

$$-(\hat{B})^2\dot{a}/r = \Lambda(\hat{B}\mathbf{e} \cdot \mathbf{m}) [ + \tilde{\Lambda}(\hat{B}\mathbf{e} \cdot \tilde{\mathbf{m}}) ] \geq 0, \quad (45)$$

where the inequality is from (42) and  $\Lambda \geq 0$  [and  $\tilde{\Lambda} \geq 0$ ]. Obviously the only possibility is that  $\hat{B} = 0$ , but that is of no interest because it would only continue beyond  $\beta$  the constant stress state of the plastic region. Thus we conclude that alternative (i) is untenable and (ii) must apply, i.e. the velocity must be discontinuous at an unloading ray  $\beta$ , from plastic to elastic, in an ideally plastic crystal. (There is no contradiction in having a reloading ray, elastic to plastic, with continuous velocity since then the

inequality reverses (42) and (45); such reloading rays appear in solutions to be presented.)

We now know that the ray at  $\beta$  must be a site of velocity discontinuity, but the earlier discussion shows that this is possible only if  $\mathbf{e}$  at  $\beta$  satisfies the flow rule condition  $\mathbf{e} \cdot \mathbf{m} = 0$  when the stress state is not at a vertex. When the stress state is at a vertex, the condition is  $\mathbf{e} \cdot (\alpha \mathbf{m} + \tilde{\alpha} \tilde{\mathbf{m}}) = 0$ , with  $\alpha \geq 0$ ,  $\tilde{\alpha} \geq 0$  and  $\max(\alpha, \tilde{\alpha}) > 0$ . But this condition can be met, while the unloading inequalities of (42) are met with  $\hat{B} \neq 0$ , only if either  $\mathbf{e} \cdot \mathbf{m} = 0$  or  $\mathbf{e} \cdot \tilde{\mathbf{m}} = 0$ .

Thus we conclude that the unloading ray is such that its direction  $\mathbf{e}$  satisfies  $\mathbf{e} \cdot \mathbf{m} = 0$  for the  $\mathbf{m}$ , or one of the  $\mathbf{m}$ s at a vertex, corresponding to the constant plastic stress state. This means that unloading rays at the growing crack tip, which are rays of velocity discontinuity (but continuous stress and displacement), occur along directions in the  $x_1, x_2$  plane which are parallel to straight-line segments of the yield surface in the  $\tau_1, \tau_2$  plane. These are the same directions of allowable discontinuities of stress and displacement for the stationary crack.

The velocity discontinuity at the unloading ray must leave behind it a discontinuously accumulated plastic strain. Consider the geometry shown in Fig. 3a. With  $[[f]] = f^- - f^+$  and noting that  $[[\gamma^e]] = 0$  since  $[[\boldsymbol{\tau}]] = 0$ , the flow rule requires that  $[[\boldsymbol{\gamma}]] = [[\boldsymbol{\gamma}^p]] = \Gamma \mathbf{m}$ , where  $\Gamma > 0$ , and the unit normal  $\mathbf{N}$  to the discontinuity is  $-\mathbf{m}$  (if  $\mathbf{m}$  is rescaled to be a unit vector). The velocity  $V$  of the discontinuity normal to itself is  $N_1 \dot{a}$ , and since by continuity of  $u$ ,

$$[[\boldsymbol{\gamma}]] \cdot \mathbf{N}V + [[\dot{u}]] = 0 \quad (\gamma_x = \partial u / \partial x_x) \quad (46)$$

we have

$$\Gamma = (\dot{u}^- - \dot{u}^+) / N_1 \dot{a}. \quad (47)$$

Now using  $N_1 = \sin \theta_0$  (Fig. 3) and observing from (28) that  $\dot{u}^-$  is logarithmically infinite at the tip, and assuming  $\dot{u}^+$  is not, one has the asymptotic result

$$\Gamma = (\hat{B} / \sin \theta_0) \ln(L/r) \quad \text{as } r \rightarrow 0, \quad (48)$$

where the scale length  $L$  is undetermined by the asymptotic analysis. (For the direction of  $\mathbf{m}$  assumed in Fig. 3, one must have  $\hat{B} > 0$ .) Thus the plastic strain accumulated discontinuously at the unloading boundary is

$$[[\boldsymbol{\gamma}^p]] = (\hat{B} \mathbf{m} / \sin \theta_0) \ln(L/r) \quad \text{as } r \rightarrow 0. \quad (49)$$

#### *Plastic sectors or elastic sectors stressed to the yield level?*

Our asymptotic analysis leads to angular sectors at a crack tip whose stress states as  $r \rightarrow 0$  meet the yield condition, typically at a vertex, and are constant in  $\theta$  within the sector. Do such sectors respond plastically or do they instead respond elastically and sustain sub-yield stress levels which meet the yield condition only at the limit point  $r = 0$ ? The complete elastic-plastic solutions developed by RICE (1967, 1984) for stationary cracks, when specialized to single crystal yield surfaces, show that the latter alternative is correct. Such sectors do in fact respond only elastically and all plasticity is confined to the displacement discontinuities separating the sectors from one another.

Further perspective, applicable to the growing crack as well, is provided by observing that a plastic zone corresponding to a vertex cannot exist over a finite angular sector at a crack tip and be bordered by elastic material that has not yet yielded. To see why, assume that such a zone did exist. The stresses  $\tau_1, \tau_2$  within it are constant, and hence they are constant along the finite arc within the sector which constitutes the elastic-plastic boundary. But for an elastically isotropic material (the argument is easily extended to anisotropy)  $\tau_2 + i\tau_1$  is an analytic function of  $x_1 + ix_2$ , and an analytic function which is constant along an arc must be constant everywhere. Hence  $\tau_1, \tau_2$  are constant everywhere, which is untenable, and we must reject the presumption that a plastic zone corresponding to a vertex can exist over a finite area, and border unyielded elastic material. The argument then suggests that constant stress sectors which are at the front of a growing crack, and which are at yield at a vertex according to the asymptotic analysis, are in fact elastic sectors which sustain a stress state that reaches yield only at the limit point  $r = 0$ . This suggestion should be borne in mind in examining asymptotic fields for growing cracks in what follows; for example, sectors  $B, B'$  in Fig. 4d are presumably elastic in the sense just discussed, as are the angular sectors immediately ahead of the growing crack for the various cases presented after that figure.

#### 4. APPLICATION TO SPECIFIC CRYSTALS AND CRACK ORIENTATIONS

In this section we will apply the asymptotic solutions developed in previous sections to different cases of crystals and the orientation of cracks within them. We will also apply the conformal mapping technique of RICE (1967, 1984) to give a full elastic-plastic small scale yielding solution for the stationary crack cases and, where possible, we will adapt an analysis by FREUND (1979) (see also FREUND and SILLS (1980)) to solve approximately for the steadily growing crack cases. In applying the yield condition (8) for the crystals and orientations which we consider here, we find that the yield surfaces in the  $\tau_1, \tau_2$  plane are diamond-shaped parallelograms. In the first case considered two edges of the parallelogram are parallel to the  $\tau_1$  axis and in the other cases vertices of the diamond are on coordinate axes.

##### *F.c.c. crystal—crack on slip plane (111), tip in slip direction $[10\bar{1}]$*

There are 12 different primary slip systems in an f.c.c. crystal, where the slip planes are octahedral planes of  $\{111\}$  type and the slip directions are face diagonals of  $\langle 10\bar{1} \rangle$  type. For the case considered in this section the crack is on the slip plane (111) and the crack tip lies along the face diagonal  $[10\bar{1}]$ . Figure 4a shows this orientation of the crystal and the crack and the corresponding yield surface is shown in Fig. 4b, with slip systems corresponding to different straight-line segments indicated. As the yield surface is the inner envelope of a set of straight lines only the four lines that are relevant are shown. Principal features of the stationary and growing crack tip fields are shown in Figs 4c and 4d, respectively.

*Stationary crack.* As already proven in detail in section 3, for the stationary crack the stress field around the crack tip will consist of sectors of constant stress type which are

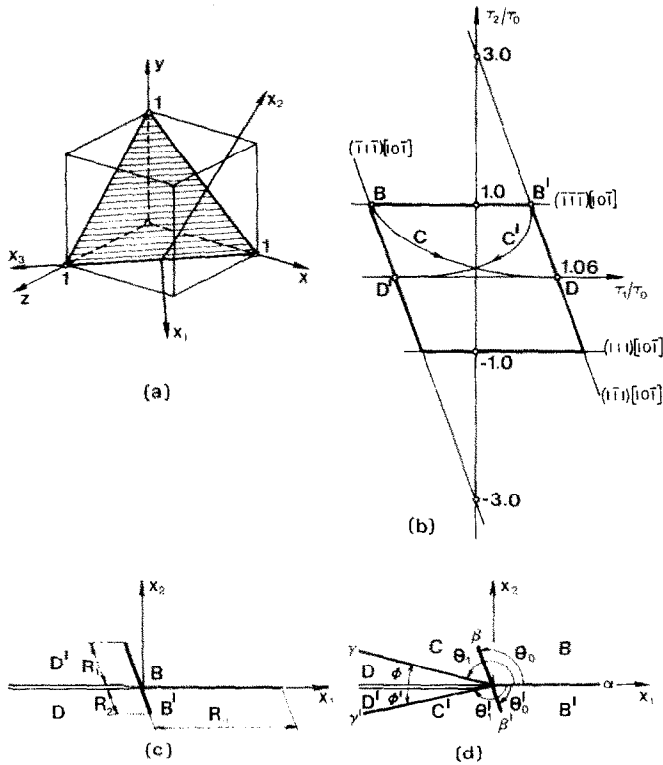


FIG. 4. (a) F.c.c. crystal with crack on (111) plane, tip along  $[10\bar{1}]$  direction, (b) the yield surface; (c) stress field around the stationary crack tip, with discontinuous changes between constant stress states at yield as  $r \rightarrow 0$ ;  $R_H, R_1, R_2$  are lengths of line plastic zones; (d) stress field around the growing crack tip;  $B, B'$ —sectors with stresses at yield;  $C, C'$ —elastic sectors;  $D, D'$ —plastic wakes;  $\alpha$ -line of displacement discontinuity,  $\beta, \beta'$ —lines of velocity discontinuities;  $\gamma, \gamma'$ —elastic to plastic interfaces. Wake angles exaggerated for clarity.

stressed to yield as  $r \rightarrow 0$ , and which are actually elastic sectors, whereas the plastic zones are the discrete lines of the displacement and stress discontinuities separating those sectors. The line plastic zones are parallel to corresponding segments of the yield surface. Line plastic zone  $R_H$  corresponds to the segment  $BB'$  of the yield surface with stresses  $\tau_1 = a\tau_0$  ( $-1.413 < a < 0.706$ ) and  $\tau_2 = \tau_0$ ; line  $R_1$  corresponds to the segment  $BD'$  with the equation  $-0.943\tau_1 - 0.333\tau_2 = \tau_0$  and line  $R_2$  corresponds to the segment  $B'D$  with the equation  $0.943\tau_1 + 0.333\tau_2 = \tau_0$ . Here  $\tau_0$  is the yield strength for any of the 12 f.c.c. slip systems. For the case of an elastically isotropic crystal in small scale yielding the lengths of these plastic zones are determined by the conformal mapping procedure in the Appendix and are

$$R_H = 0.385(K^2/\tau_0^2), \quad R_1 = 0.202(K^2/\tau_0^2), \quad R_2 = 0.076(K^2/\tau_0^2);$$

the displacement discontinuity at the crack tip is

$$\Delta u = 0.584(K^2/\mu\tau_0).$$



Thus we have for stresses in sectors  $B$  and  $B'$

$$\tau_1 = -1.413\tau_0, \quad \tau_2 = \tau_0 \quad \text{in } B, \quad (50a)$$

$$\tau_1 = 0.707\tau_0, \quad \tau_2 = \tau_0 \quad \text{in } B', \quad (50b)$$

and the line ahead of the crack remains a line plastic zone of stress and displacement discontinuity (permissible since  $h_1 = 0$  on that line). The interfaces  $\beta$  and  $\beta'$  satisfy conditions required for plastic to elastic interfaces in section 3 and are parallel to corresponding segments of the yield surface  $BD'$  and  $B'D$ , respectively (Fig. 4b and d). Now using (27), again treating the elasticity as isotropic, we can write the stress continuity condition across  $\beta$ , at  $\theta = \theta_0 = 109.46^\circ$ ,

$$\tau_1 = -1.413\tau_0 = C - B \ln(\sin \theta_0), \quad \tau_2 = \tau_0 = A - B\theta_0. \quad (51)$$

A similar set of equations can be written for the lower part of the field. Thus we obtain the final expressions for stresses in elastic regions as

$$\tau_1 = -1.413\tau_0 - B \ln(\sin \theta / \sin \theta_0), \quad \tau_2 = \tau_0 - B(\theta - \theta_0) \quad \text{in } C \quad (52a)$$

and

$$\tau_1 = 0.707\tau_0 - B' \ln(\sin \theta / \sin \theta'_0), \quad \tau_2 = \tau_0 + B'(\theta - \theta'_0) \quad \text{in } C', \quad (52b)$$

where  $C$  and  $C'$  are the elastic sectors respectively above and below the crack tip in Fig. 4d, and constants  $B$  and  $B'$  are yet to be determined.

Stresses in the elastic region vary with  $\theta$  (following the path  $C$  or  $C'$  of Figs 4b and 5) but the elastic sector cannot extend up to  $\theta = \pi$ , i.e. to the crack surface, because the expressions for  $\tau_1$  would then be unbounded. The crack surface boundary condition is  $\tau_2 = 0$  and this condition can be met at points  $D$  and  $D'$  of the yield surface (Figs 4b and 5). Thus, we join the elastic sectors to constant stress sectors  $D$  and  $D'$  in Fig. 4d, i.e. plastic wakes with

$$\tau_1 = 1.06\tau_0, \quad \tau_2 = 0 \quad \text{in } D \quad \text{and} \quad \tau_1 = -1.06, \quad \tau_2 = 0 \quad \text{in } D'.$$

Thus we have elastic to plastic interfaces  $\gamma$  and  $\gamma'$  which, according to section 3, can exist and have velocity continuity. We now impose the stress continuity condition across  $\gamma$ , the interface between elastic sector  $C$  and plastic wake  $D$ , which will allow us to solve for the constant  $B$  and angle of the interface  $\theta_1$  (or the angle of the wake  $\Phi$  where  $\Phi = \pi - \theta_1$ ); Fig. 4d. Thus, for  $\theta = \theta_1$ ,

$$\tau_1 = 1.06\tau_0 = -1.413\tau_0 - B \ln(\sin \theta_1 / \sin \theta_0), \quad (53a)$$

$$\tau_2 = 0 = \tau_0 - B(\theta_1 - \theta_0). \quad (53b)$$

From (53b) we can express  $B$  in terms of  $\tau_0$ ,  $\tau_2$  and  $\theta_0$  and  $\theta_1$  and substitute into (53a), to obtain the equation for  $\Phi$

$$2.417(\pi - \theta_0) - 2.417\Phi = -\ln(\sin \Phi) + \ln(\sin \theta_0). \quad (54)$$

We can obtain similarly the equation for the angle of the lower wake. They have solutions

$$\Phi = 0.0509 \text{ rad} = 2.91^\circ \quad \text{and} \quad \Phi' = 0.0343 \text{ rad} = 1.96^\circ.$$

Corresponding values of the constants are

$$B = \tau_0/(\theta_1 - \theta_0) = \tau_0/(\pi - \Phi - \theta_0) = 0.847\tau_0 \quad \text{and} \quad B' = 0.533\tau_0.$$

From (49) with  $\hat{B} = B/\mu$ , the plastic strain accumulated at the velocity discontinuity at  $\beta$  is of the form

$$\gamma^p = (B/\mu \sin \theta_0) \mathbf{m}^{(1)} \ln(L/r) \quad \text{as} \quad r \rightarrow 0 \quad (55)$$

and this plastic strain prevails throughout the elastic region  $C$ , so long as  $r$  is interpreted as the radius of a material point when it is traversed by the moving discontinuity  $\beta$ .

Further plastic straining, in addition to the Dirac-singular  $\gamma^p_2$  accumulated on  $x_2 = 0$  in the front discontinuity, occurs in the wake  $D$  and there the flow rule requires  $\dot{\gamma} = \dot{\gamma}^p = \Lambda \mathbf{m}^{(2)}$  (note that  $\dot{\gamma}^e$  vanishes in the wake). Thus by (9), in the wake,

$$\dot{u} = f(\mathbf{x} \cdot \mathbf{m}^{(2)}), \quad \Lambda = f'(\mathbf{x} \cdot \mathbf{m}^{(2)}) \geq 0. \quad (56)$$

Since  $\dot{u}$  must be continuous across the boundary of the wake at  $\gamma$  in Fig. 4d, so also must  $\mathbf{e} \cdot \dot{\gamma}$ . This is given on the elastic side of the boundary by (40) and setting  $\mathbf{x} = r\mathbf{e}_r$ , along that boundary ( $\mathbf{e}_r$  is the radial unit vector at  $\theta_1$ ), there results for  $r \rightarrow 0$

$$f'(r\mathbf{e}_r \cdot \mathbf{m}^{(2)}) = -B\dot{a}/\mu r. \quad (57)$$

Note that  $\mathbf{e}_r \cdot \mathbf{m}^{(2)} < 0$ . Thus the function  $f'(\lambda)$  is such that

$$f'(\lambda) = -B\dot{a}/\mu\lambda, \quad \lambda \rightarrow 0$$

and hence  $f(\lambda) = (B\dot{a}/\mu) \ln(\bar{L}/|\lambda|)$  where the scaling length  $\bar{L}$  is undetermined by the asymptotic analysis. Finally,

$$\dot{u} = (B\dot{a}/\mu) \ln(\bar{L}/|\mathbf{x} \cdot \mathbf{m}^{(2)}|) \quad (58)$$

in the wake near the crack tip, and this shows that the upper crack face velocities have the form

$$\dot{u} = (B\dot{a}/\mu) \ln(\bar{L}/r), \quad r \rightarrow 0, \quad (59)$$

where  $\bar{L} = \bar{L}/|m_1^{(2)}|$ .

Equations similar to (56), (58) and (59) can be derived for the lower field in Fig. 4d. In this case we have not been able to proceed further to develop a complete small scale yielding solution, but this can be done approximately for other growing crack cases to be considered next.

#### *F.c.c. crystal—crack on cube face plane (010), tip in slip direction [10 $\bar{1}$ ]*

This, and two following subsections deal with cases for which the yield surface is a diamond with vertices on the  $\tau_1, \tau_2$  axes. This form is obtained for both f.c.c. and b.c.c. crystals when the crack is on the (010) cube face plane. For the particular case considered in this subsection the crack and crystal orientations as well as the shape of the yield surface is shown in Fig. 6, where the near tip stress field solutions for both stationary and growing crack are also illustrated. Owing to the symmetry of the yield surface the stress field is symmetric about the crack line.

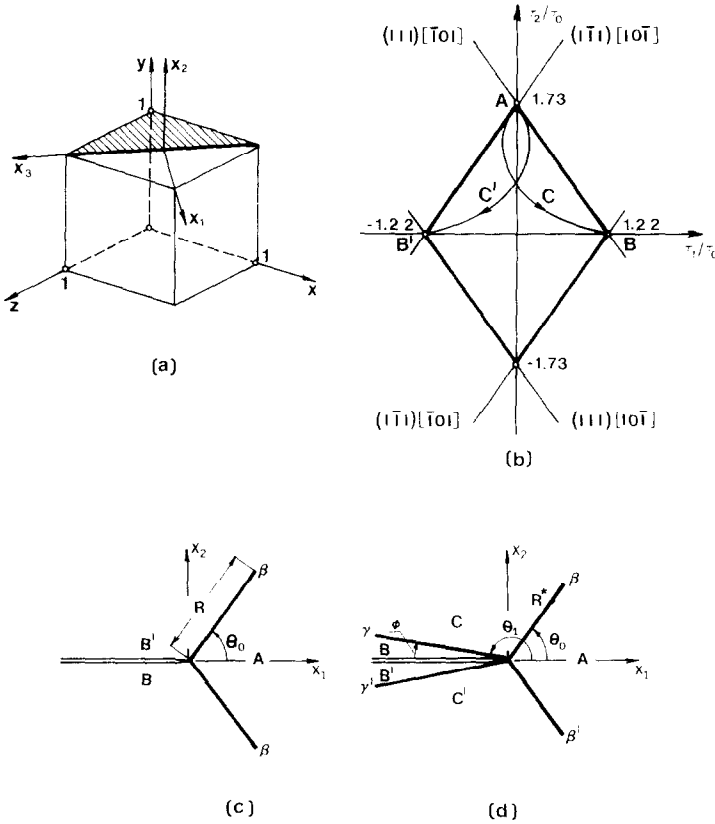


FIG. 6. (a) F.c.c. crystal with crack on (010) plane, tip along  $[10\bar{1}]$  direction; (b) the yield surface; (c) stress field around the stationary crack tip;  $R$  is length of line plastic zones; (d) stress field around the growing crack tip:  $A$  - sector with stresses at yield;  $B, B'$  - plastic wakes;  $C, C'$  - elastic sectors;  $\beta, \beta'$  - lines of velocity discontinuities;  $\gamma, \gamma'$  - elastic to plastic interfaces.

*Stationary crack.* The results are illustrated in Fig. 6c. Constant stress states at vertices  $A, B', B$  are separated by line plastic zones. The conformal mapping procedure as explained in the Appendix enables us to determine the lengths of the line plastic zones as  $R = 0.292 (K^2/\tau_0^2)$  and the displacement discontinuity at the crack tip is  $\Delta u = 0.346 (K^2/\mu\tau_0)$ .

*Growing crack.* The procedure of obtaining the solution for the growing crack is somewhat different than for the case in Figs 4 and 5. Here we do not have the line of displacement discontinuity,  $\alpha$ , ahead of the crack tip (no corresponding horizontal segment on the yield surface), but the sector  $A$  with constant stresses at yield results over  $-\theta_0 < \theta < +\theta_0$ , where  $\theta_0 = 0.9553 \text{ rad} = 54.74^\circ$  is the slope of the inclined faces of the diamond (Fig. 7). The sector ends at the lines of velocity discontinuity  $\beta$  at angle  $\theta_0$ , beyond which there is an elastic sector. Now, knowing this angle we can calculate the position of lines  $\gamma$ , i.e. the interfaces between the elastic sectors  $C, C'$  and plastic

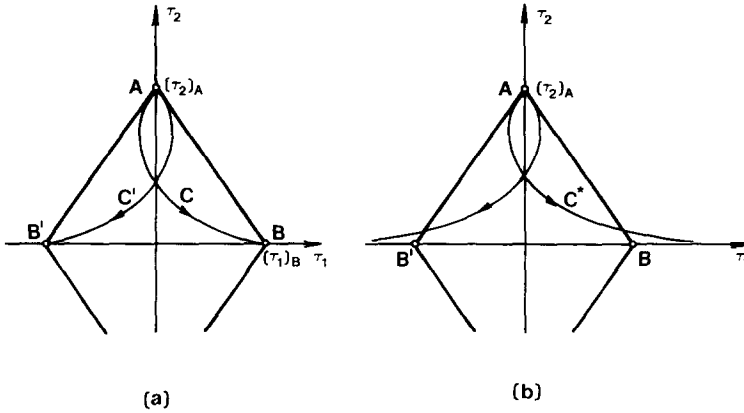


FIG. 7. (a) Yield surface of Fig. 6b and stress trajectory in elastic sector; (b) stress trajectory of Freund procedure (1979) for  $\theta_0 = 54.74^\circ$ .

wakes  $B, B'$ , respectively. As we start from the point  $A$  of the yield surface the stresses in sector  $A$  will be

$$\tau_1 = 0, \quad \tau_2 = (\tau_2)_A. \tag{60}$$

From stress continuity across  $\beta$  we obtain for stresses in the elastic region  $C$

$$\tau_1 = -B \ln(\sin \theta / \sin \theta_0), \tag{61a}$$

$$\tau_2 = (\tau_2)_A - B(\theta - \theta_0), \tag{61b}$$

with  $(\tau_2)_A = 1.732\tau_0$  for the present case. Figure 7a shows the procedure of obtaining the angle  $\theta_1$  at which the interface  $\gamma$  occurs between the elastic sector  $C$  and plastic wake  $B$ . Starting from point  $A$  the stress trajectory of (61) departs from the yield surface tangentially and follows a path  $C$  throughout the elastic region. The constant  $B$  in (61) must be chosen so that the trajectory passes to the stress state at vertex  $B$  in Fig. 7a so as to meet the crack surface boundary condition. Since  $(\tau_1)_B = (\cos \theta_0 / \sin \theta_0)(\tau_2)_A$  we will have

$$\tau_1 = (\cos \theta_0 / \sin \theta_0)(\tau_2)_A = -B \ln(\sin \theta_1 / \sin \theta_0), \tag{62a}$$

$$\tau_2 = 0 = (\tau_2)_A - B(\theta_1 - \theta_0). \tag{62b}$$

Eliminating  $B$ , we can solve for the angle  $\theta_1$  at the wake interface  $\gamma$ , and the angle of the wake  $\Phi$ , where  $\Phi = \pi - \theta_1$ , is given by

$$(\pi - \Phi - \theta_0)(\cos \theta_0 / \sin \theta_0) = \ln(\sin \theta_0) - \ln(\sin \Phi). \tag{63}$$

Substituting the value for  $\theta_0$ , we obtain for the wake angle  $\Phi = 0.201 \text{ rad} = 11.52^\circ$ . The corresponding value of the constant is  $B = 0.872\tau_0$ .

We can solve approximately for the length of the inclined plastic zone (velocity discontinuity at  $\beta$ ), at least for steady state crack growth under small scale yielding conditions, by adapting a result by FREUND (1979). As an approximate model for yield at a growing anti-plane crack tip, presumably in an isotropic material, he assumed that

all plastic flow occurred along two straight lines of velocity discontinuity emanating from the crack tip at angles  $\pm\theta_0$  ( $\theta$  in his notation and determined the length of these lines as well as the distribution of velocity discontinuity (hence plastic strain accumulation; see equation (49)) along them by requiring that the stress component  $\tau_\theta = \tau_y$ , is constant, along them. As we see Freund's assumptions describe the situation in crystals with diamond-shaped yield surfaces as in Figs 6 and 7, the only difference is that he does not include the wake. That is, Freund's elastic sector, beyond  $\theta_0$ , extends all the way to the crack surfaces at  $\theta = \pi$ , and the parameter  $B$  in the equation (61) is then chosen in his elastic sector to meet the crack surface boundary condition. Thus, the stresses in his elastic sector are

$$\tau_1 = -[(\tau_2)_A/(\pi - \theta_0)] \ln(\sin \theta / \sin \theta_0), \quad (64a)$$

$$\tau_2 = (\tau_2)_A(\pi - \theta)/(\pi - \theta_0) \quad (64b)$$

and he commented explicitly on the logarithmic divergence of the expression for  $\tau_1$ . Freund's stress distribution is identical to that of equations (61), but with the exact  $B = 0.872\tau_0$  for this case replaced by  $0.791\tau_0$ . Figure 7b shows a plot of the stress trajectory according to Freund's analysis. This is, in fact, the worst case of those we consider. The next case involves a much smaller wake angle and, as might be expected, the Freund trajectory is then much closer to the actual trajectory.

Hence, to within the approximation of neglecting the plastic flow in the wake Freund's solution may be used to estimate the size of the plastic zone at  $\beta$ . Reading results for  $\theta_0 = 54.74^\circ$  from Fig. 3 of his 1979 paper and setting  $\tau_y = \tau_0$  we obtain  $R^* = 0.144 (K^2/\tau_0^2)$  for steady state quasistatic crack growth under small scale yielding in the crystal geometry considered. This is considerably smaller than the result noted earlier for the stationary crack.

We have not been able to work out unique results for the near tip plastic strain rate in the wake since the stress state there corresponds to a vertex. However, it is interesting to note that if the yield surface were very slightly rounded at vertex  $B$ , a virtually identical near tip distribution would result but the direction of plastic flow in the wake would be unique, with  $\dot{\gamma} = \dot{\gamma}^p = \Lambda \mathbf{i}_1$ , where  $\mathbf{i}_1$  is a unit vector in the  $x_1$  direction and (then) the normal to the yield surface at  $B$ . Thus the analysis of equations (57)–(59) applies directly to this case with  $\mathbf{e}_y$  now understood to correspond to the present direction  $\gamma$  at angle  $\theta_1$ ,  $B$  to the present  $B$ , and with  $\mathbf{m}^{(2)}$  replaced everywhere in those equations by  $\mathbf{i}_1$ .

*F.c.c. crystal—crack on cube face plane (010), tip in cube edge direction [001]*

For this case of orientation of the crack we also obtain the diamond, reduced to a square, with vertices on the  $\tau_1, \tau_2$  axes for the yield surface. This case is interesting because we have simultaneously active two slip systems along each straight-line segment and four systems at each vertex. This is shown schematically in Fig. 8, where the figure of crystal, and stationary, and growing crack solutions are also illustrated, and the nature of the double slip corresponding to each straight-line segment of the yield surface is shown. In contrast to the previous cases, here the line (or plane, in three dimensions) plastic zones emanating from the tip do not coincide with a crystal slip

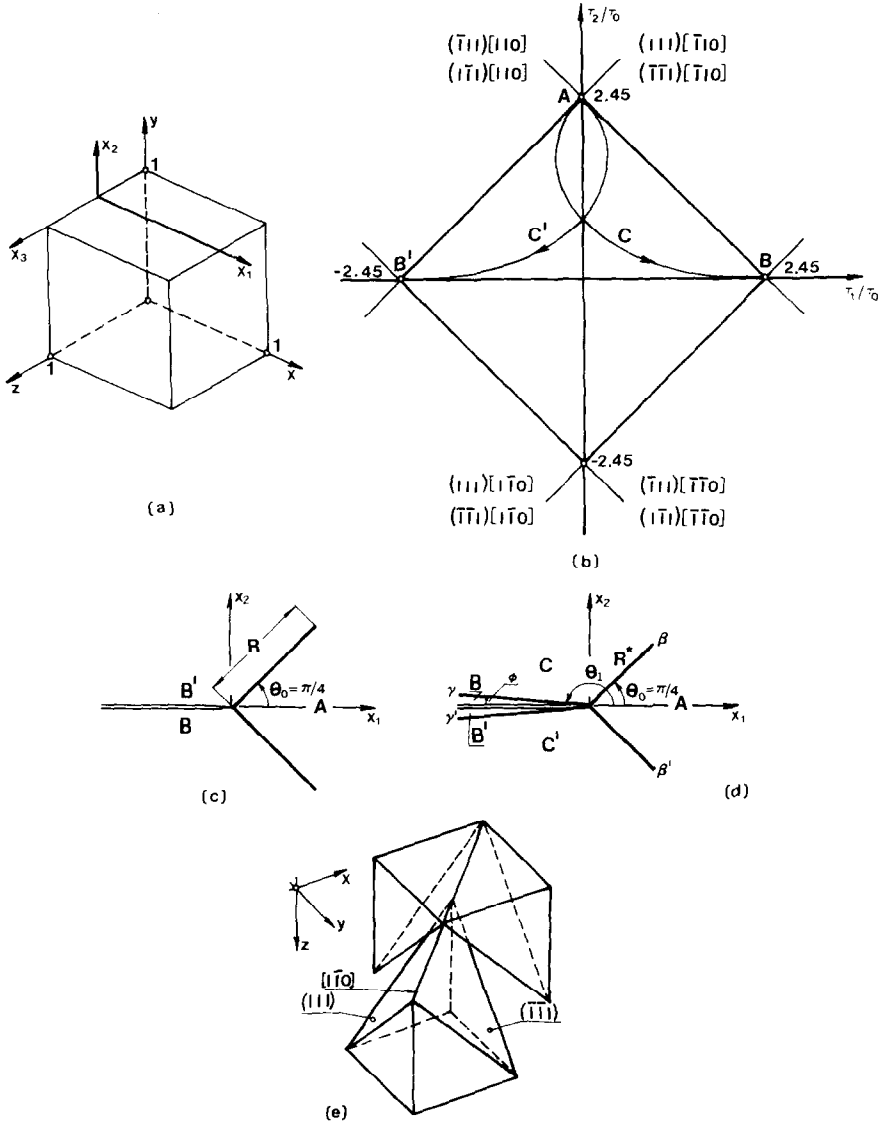


FIG. 8 (a) F.c.c. crystal, crack on (010) plane, tip along [001] direction; (b) the yield surface; (c) stress field around the stationary crack tip; (d) stress field around the growing crack tip; (e) simultaneous slip on two slip planes.

plane. In Fig. 8b, the distance  $\tau_y$  of the straight-line yield surface segments from the origin is  $1.732\tau_0$ .

*Stationary crack.* The solution, obtained by the conformal mapping procedure given in the Appendix, for the lengths of plastic zones and displacement discontinuity at the crack tip is  $R = 0.104(K^2/\tau_0^2)$  and  $\Delta u = 0.198(K^2/\mu\tau_0)$ .

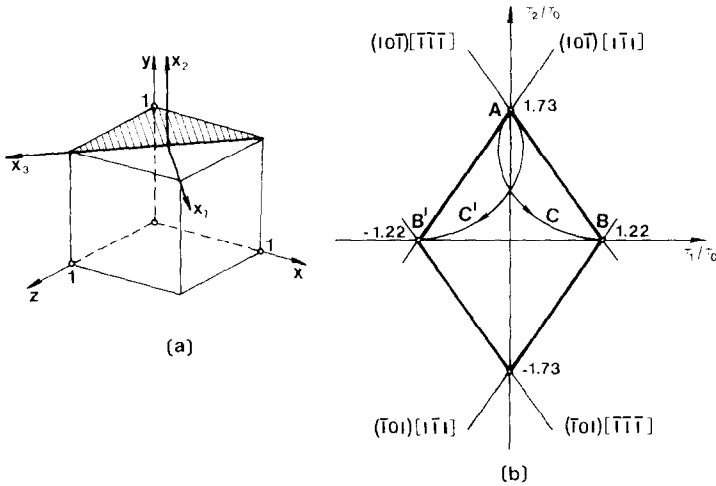


FIG. 9. (a) B.c.c. crystal; crack on (010) plane, tip along  $[10\bar{1}]$  direction. (b) The yield surface (same as in Fig. 6; solution same as in Fig. 6c and d).

*Growing crack.* The procedure for obtaining the solution is given in the previous subsection. The results are angles  $\theta_0 = 0.785$  rad =  $45^\circ$ ,  $\Phi = 0.0729$  rad =  $4.130^\circ$ , constant  $B$  in expressions for stresses given as  $B = 1.073\tau_0$  (versus  $1.039\tau_0$  in the Freund procedure) and the length of the line plastic zones estimated from the Freund procedure as  $R^* = 0.056(K^2/\tau_0^2)$ .

#### *B.c.c. crystal—crack on cube face plane (010), tip in slip direction $[\bar{1}01]$*

The crack orientation is shown in Fig. 9a. It is the same, relative to the unit cube, as the f.c.c. case in Fig. 6, but now the crack tip does not coincide with a slip direction.

In b.c.c. crystals there can be several types of slip systems as  $\{110\}\langle\bar{1}\bar{1}1\rangle$ ,  $\{112\}\langle 11\bar{1}\rangle$  and  $\{123\}\langle 11\bar{1}\rangle$ . We calculated the resolved shear stress for these three different types of slip systems. If we assume, following HONEYCOMBE (1961), that  $\tau_0$  is the same for all slip systems then the inner envelope defining the yield surface is formed only by systems of the first type. The result is shown in Fig. 9b, and the yield surface is found to be identical to that for the f.c.c. case in Fig. 6b, except that now  $\tau_0$  is the b.c.c. critical yield strength for  $\{110\}\langle\bar{1}\bar{1}1\rangle$ . Since the yield surface is the same, it follows within our present ideally plastic modelling that the solution and all numerical values which enter it are fully identical to what is shown in Fig. 6c and d and discussed in section 4.

This is an interesting case because the slip systems which determine the yield surface, and hence relax the crack, all have as their slip plane the (10 $\bar{1}$ ) plane, which is the plane perpendicular to the crack tip, i.e. it is the plane of type  $x_3 = \text{constant}$  and hence the plane of such Fig. as 6c and d. Thus, in this case the planar plastic zones which emanate from the crack tip are actually *perpendicular* to the crystal slip plane which is active. In fact, for this b.c.c. case the crack tip is parallel to the normal  $\mathbf{n}$  to the activated crystal

slip plane, whereas the line traces (in the  $x_1, x_2$  plane) of the plastic zones are perpendicular to the activated slip directions  $\mathbf{s}$ . By contrast, for the f.c.c. case of Fig. 6, the crack tip is parallel to the activated slip direction  $\mathbf{s}$ , whereas the line traces of the plastic zones are perpendicular to the normal  $\mathbf{n}$  of the activated crystal slip planes.

The comparison emphasizes a symmetry in the ideal plasticity formulation for crystals which is perhaps seldom contemplated. In particular, the yield condition and hence ideally plastic response of a slip system with parameters  $\mathbf{n} = \mathbf{a}$ ,  $\mathbf{s} = \mathbf{b}$  is indistinguishable within the continuum theory from that of another system with parameters  $\mathbf{n} = \mathbf{b}$ ,  $\mathbf{s} = \mathbf{a}$ . It is just such an interchange, with  $\mathbf{a} = (1, 1, 1)$  and  $(1, -1, 1)$ ,  $\mathbf{b} = (-1, 0, 1)$ , which converts the case in Fig. 6 to that in Fig. 9. It may be noted that while the yield condition and flow rule are unaffected by  $\mathbf{n}, \mathbf{s}$  interchange, the rotation of the underlying crystal lattice directions relative to the material reverse sign under such interchange. Thus a continuum plasticity formulation which accounts for geometrical hardening or softening due to rotation of the crystal planes and directions for which resolved shear stresses are calculated (such effects are not included in "small strain" formulations) will not be symmetric under interchange of  $\mathbf{n}$  and  $\mathbf{s}$ .

## 5. CONCLUDING DISCUSSION

We have considered quasistatic crack problems in ideally plastic single crystals oriented so that anti-plane shear is a possible deformation state. The yield surface in the two-dimensional  $\tau_1, \tau_2$  plane is then a convex polygon, given as the inner envelope of the straight lines of various orientations representing critical shearing on different crystal slip systems. The envelope was diamond-shaped for the specific crystals and crack orientations considered here, but this is not always the case and two examples are cited below for which the yield surface is a regular hexagon.

The solutions developed for stationary cracks, subject to monotonic load increase, show that all plastic flow near the crack tip is confined to planar plastic zones emanating from and containing the crack tip. The planar zones have orientations in the  $x_1, x_2$  plane parallel to those of the activated straight-line segments of the yield surface in the  $\tau_1, \tau_2$  plane. These plastic zones are surfaces across which both displacement and stress (specifically, component  $\tau_x$ ) are discontinuous.

We have inferred the existence of such planar plastic zones here on the basis of a direct analysis for a polygonal yield surface. However, the anti-plane shear formulation can be given in some generality for stationary cracks in anisotropic ideally plastic materials (RICE, 1967, 1984), and visualization of the solution is aided by a simple membrane analogy. On this basis it is possible to assert that the solutions given here with their planar plastic zones and associated discontinuities are also interpretable as a well defined limit as  $\varepsilon \rightarrow 0$  of the solution for another material model, parameterized by  $\varepsilon$ , for which the plastic zones are diffuse and displacement and stress are fully continuous when  $\varepsilon > 0$ . Here  $\varepsilon$  represents a small curvature convex relative to the origin in the  $\tau_1, \tau_2$  plane given to each formerly straight-line segment of the yield surface. For the material thus defined, with  $\varepsilon > 0$ , the plastic zone consists of diffuse lobes emanating from the crack tip. But as  $\varepsilon \rightarrow 0$ , each lobe contracts continuously into a plane and gradients in the displacement and stress fields steepen into discontinuities

across that plane. The discontinuous solutions given here coincide also with what one would calculate following the anti-plane version of the well known procedure of BILBY, COTTRELL and SWINDEN (1963). There, one assumes *a priori* that the plastic zone consists of planes of displacement discontinuity emanating from the tip across which a critical shear stress acts. The lengths of these zones are chosen such that no stress singularities occur at their outer edges. If the orientations of the planes and the critical stresses are correctly chosen, the exact continuum plasticity solutions as given here would be duplicated by that procedure. The procedure of Bilby *et al.* is normally described as one of using continuously distributed dislocations on a plane, or planes, to represent the plasticity, and in the anti-plane cases the surrounding elastic field can be thought of as having been generated by a continuous distribution of screw dislocations with axes parallel to the crack tip. As the subsequent discussion indicates, the actual crystal dislocations involved in the plastic relaxation can be reasonably assumed to be of the same screw type for some crack orientations, notably those for which the crack tip lies in a crystal slip plane, but not for others.

The solutions developed here for quasistatically growing cracks in ideally plastic crystals are necessarily such that the displacement and stress fields are fully continuous, at least off of the crack plane and its prolongation. For the growing crack too we find that apart from reverse flow plastic wakes along the crack surfaces, all active plasticity takes place in planar plastic zones emanating from and containing the crack tip. These planar zones have the same orientations relative to the activated straight-line segments of the yield surface, as described above for the stationary crack. The plastic zones are planes across which the velocity of material particles is discontinuous, and as these planes sweep over a material point a plastic strain is accumulated discontinuously there. We were not able to develop exact full solutions for the size of plastic regions in this case, but could do so approximately for steady state crack growth with small scale yielding in some of the cases considered here (Figs 6–9) by adapting previous work by FREUND (1979).

We presented two examples of cracked f.c.c. crystals for which the planar plastic zones corresponded with crystal slip planes (Figs 5 and 6), one for a f.c.c. crystal for which the planar zones involved multi-slip and did not lie on slip planes (Fig. 8), and one for a b.c.c. crystal for which the planar plastic zones were perpendicular to a crystal slip plane (Fig. 9). It is of course possible to find crack orientations in a b.c.c. crystal such that a planar plastic zone coincides with a crystal slip plane, such as occurs directly ahead of the crack tip when the tip lies along  $[10\bar{1}]$  as in Fig. 9 but when the crack plane normal is instead  $[101]$ . Also, it occurs whenever the tip lines along  $[111]$ , a b.c.c. slip direction, and in that case the yield surface in the  $\tau_1, \tau_2$  plane is a regular hexagon. Similarly, one can find crack orientations in f.c.c. crystals for which a planar plastic zone is perpendicular to a crystal slip plane. This occurs, for example, when the crack tip lies along  $[111]$ , a f.c.c. slip plane normal, and in this case too the yield surface is a regular hexagon. Indeed this and the last b.c.c. case mentioned constitute an example of symmetry of the ideally plastic solution under interchange of  $\mathbf{n}, \mathbf{s}$  for  $\mathbf{s}, \mathbf{n}$  as mentioned at the close of section 4.

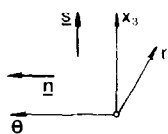
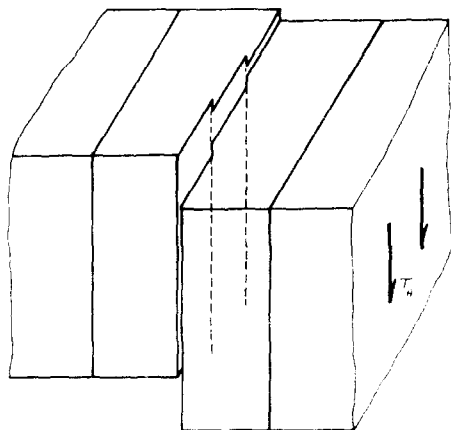
It will be of interest to seek experimental evidence for the type of concentrated plastic flow predicted, to study theoretically the effects of material strain hardening (actual and geometric) and inertia on the predictions, and to seek the correspondence between the

present continuum plasticity solutions for crystals and the arrays of lattice dislocations forming at a crack tip.

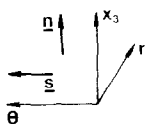
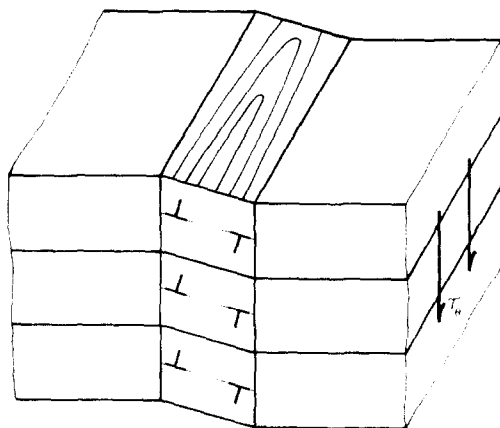
As regards the latter correspondence, a tacit hypothesis of the continuum approach is that potential sources, from which new dislocation loops may be generated, are pervasive over the size scale of interest. Here, the size scale is that of the crack tip plastic zone which, according to solutions like those presented, may be arbitrarily small depending on the level of the applied load and, even at load levels that would be appropriate for crack advance (were the loading not in shear), may still not be large compared to source spacing in the more brittle crystals. Clearly, a material element can deform plastically (at stresses typical of macroscopic yield) only if it contains sources or if an ample supply of dislocations generated elsewhere can move into that element. Thus, when the plastic zone develops along a crystal slip plane, dislocations sweeping out from what would otherwise be a highly stressed crack tip may obviate the necessity for pervasive sources. By contrast, when the predicted plastic zone develops perpendicular to a slip plane, there is no similar way of sweeping dislocations out along the plastic zone and, in the absence of pervasive sources, a result corresponding closely to what is predicted here may not occur.

The dislocation structures corresponding to these two cases are sketched in Fig. 10 where a cut perpendicular to the plastic zone is shown. The direction of the crack tip, along  $x_3$ , is vertical in these figures and corresponds to  $\mathbf{s}$  in the first case, Fig. 10a, and to  $\mathbf{n}$  in the second, Fig. 10b. In each case  $r$  denotes the direction outwards from the crack tip and  $\theta$  the direction perpendicular to the planar plastic zone. The  $\theta$  direction coincides with  $\mathbf{n}$  in the first case and  $\mathbf{s}$  in the second. As illustrated in Fig. 10a, the loops generated on or near a single slip plane are expected to be the kinematic equivalent of an array of screw dislocations lying parallel to the crack tip. There is no rotation of the slip planes and hence no basis for geometrical hardening or softening in this case. These screw dislocations, or actual loops, will not all be on the same plane if many sources are activated, or if some of the screw segments cross-slip. In the absence of sources, it is possible that all dislocations of the array are nucleated from the crack tip. Such has been seen in electron microscope studies of cracks in thin, tensile-loaded foils of b.c.c. and f.c.c. metals (OHR and NARAYAN, 1980; KOBAYASHI and OHR, 1980, 1981; OHR and CHANG, 1982). In these studies the cracks were initiated at the edge of a hole formed by chemical thinning of the foil and apparently began by complete slipping off along a crystal plane tilted at approximately  $45^\circ$  to the plane of the foil, with plasticity occurring as a screw dislocation array like that in Fig. 10a along the prolongation of the cracked slip plane.

The case shown in Fig. 10b, however, is one in which sources emit dislocation loops in planes perpendicular to the crack tip. To accomplish the concentrated shear, the dislocation array is then expected to be the kinematic equivalent of highly elongated loops of predominantly edge character. The resulting walls of edge dislocations accomplish the shear by effectively forming two tilt boundaries of opposite sense. This involves a rotation of the slip planes as shown and hence is expected to involve strong geometrical hardening. Both cases are identical within the ideally plastic model, but we expect that both the lattice rotation and the width required for the accommodating array of loops, Fig. 10b, will make the actual thickness of the "planar" plastic zone much greater in the latter case.



(a)



(b)

FIG. 10. Dislocation structures corresponding to planar plastic zones of concentrated shear : (a) slip direction  $s$  is along crack tip and plastic zone lies on slip plane ; (b) slip plane normal  $n$  is along crack tip and plastic zone is perpendicular to slip plane.

Yet another aspect of discrete dislocation effects at the crack tip involves the "dislocation free zone" of CHANG and OHR (1981) for cases like that in Fig. 10a. The observations mentioned of crack tips in foils suggested that the relaxing dislocation arrays were somewhat detached from the crack tip where they were nucleated. Chang and Ohr argued that this can be explained on the basis that a critical elastic stress intensity factor must be achieved within the slipped but elastic and dislocation-line-free near tip region to nucleate yet another dislocation from the tip, and have derived in this way estimates of the dislocation-free zone size. These estimates are comparable to observed values, although three-dimensional complexities of the slant fractures in the foils are not included in their two-dimensional anti-plane modelling.

#### ACKNOWLEDGEMENT

This study was supported by the U.S. National Science Foundation through the Materials Research Laboratory at Harvard University. R. Nikolic was supported additionally by the International Research and Exchange Program.

#### REFERENCES

- BILBY, B. A., COTTRELL, A. H. and SWINDEN, K. H. 1963 *Proc. Roy. Soc. Lond.* **A272**, 304
- CHANG, S.-J. and OHR, S. M. 1981 *J. appl. Phys.* **52**, 7174.
- CHITALEY, A. D. and MCCLINTOCK, F. A. 1971 *J. Mech. Phys. Solids* **19**, 147.
- DRUGAN, W. J. and RICE, J. R. 1984 *Mechanics of Material Behavior*, D. C. Drucker Anniversary Volume (edited by G. J. DVORAK and R. T. SHIELD), p. 59. Elsevier, Amsterdam.
- FREUND, L. B. 1979 *Nonlinear and Dynamic Fracture Mechanics: AMD—Vol. 35* (edited by N. PERRONE and S. N. ATLURI), p. 171. ASME, New York.
- FREUND, L. B. and SILLS, L. B. 1980 *J. Mech. Phys. Solids* **28**, 49.
- HONEYCOMBE, R. W. K. 1961 *Prog. Mater. Sci.* **9**, 93.
- KOBAYASHI, S. and OHR, S. M. 1980 *Phil. Mag.* **A42**, 763.
- KOBAYASHI, S. and OHR, S. M. 1981 *Scripta Met.* **15**, 343.
- OHR, S. M. and NARAYAN, J. 1980 *Phil. Mag.* **A41**, 81.
- OHR, S. M. and CHANG, S.-J. 1982 *J. appl. Phys.* **53**, 5645.
- RICE, J. R. 1967 *Fatigue Crack Propagation*, ASTM-STP 415, p. 247. American Society for Testing and Materials, Philadelphia.
- RICE, J. R. 1982 *Mechanics of Solids* (edited by H. G. HOPKINS and M. J. SEWELL), p. 539. Pergamon Press, Oxford.
- RICE, J. R. 1984 *Mech. Mater.* **3**, 55.

#### APPENDIX

Here we give a brief explanation of the conformal mapping procedure with which we obtained results for the stationary crack for different cases quoted in section 4. RICE (1967, 1984) developed

this procedure to give the anti-plane small scale yielding solution for an ideally plastic material with an arbitrarily anisotropic but convex yield surface, with an associated flow rule, and with isotropic elastic response. He gave the solution in terms of the analytic function  $\Omega(\tau)$ , with  $\tau = \tau_1 + i\tau_2$ , which conformally maps the upper portion of the sub-yield stress domain (i.e. a region bounded by portion of yield surface with  $\tau_2 \geq 0$  and by  $\tau_1$  axis) into the upper portion of a unit circle in the complex  $\Omega$  plane. The map is constrained such that intersections of the yield surface with the negative and positive  $\tau_1$  axis map to  $-1$  and  $+1$ , respectively, on the  $\text{Re}(\Omega)$  axis, and that  $\tau = 0$  maps to  $\Omega = 0$ . Hence the  $\tau_1$  axis maps to the  $\text{Re}(\Omega)$  axis, and for points  $\tau$  on the upper part of the yield surface

$$\Omega(\tau) = e^{i\Phi} = i e^{i\psi},$$

where  $\Phi, \psi$  are angles measured anti-clockwise from the positive  $\text{Re}(\Omega)$  and  $\text{Im}(\Omega)$  axes, respectively, to points on the unit circle  $|\Phi| = 1$  and  $0 \leq \Phi \leq \pi, -\pi/2 \leq \psi \leq \pi/2$ . The same function  $\Omega(\tau)$  maps the upper portion of the sub-yield domain and its mirror image about the  $\tau_1$  axis to the full unit circle in the  $\Omega$  plane.

The small scale yielding problem may be regarded as that of a semi-infinite crack in an infinite body with asymptotic boundary conditions

$$\lim_{r \rightarrow \infty} (\tau_1 + i\tau_2) \rightarrow K/[2\pi(x_1 + ix_2)]^{1/2} \tag{A.1}$$

for coordinates  $x_1, x_2$  centered at the crack tip. For this problem, RICE (1984) (equation 71) shows that the solution for coordinates  $x_1, x_2$  of points within the elastic region corresponding to sub-yield stress  $\tau$ , is

$$x_1 - ix_2 = [\Omega'(0)K^2/2\pi]\Omega'(\tau) [1 - 1/\Omega^2(\tau)]. \tag{A.2}$$

Our conformal maps for single crystal yield surfaces are obtained by the Schwarz-Christoffel method and hence are more naturally expressed in the form  $\tau = \tau(\Omega)$ , rather than  $\Omega = \Omega(\tau)$ . Thus

$$x_1 - ix_2 = [K^2/\pi\tau'(0)] [i/\Omega\tau'(\Omega)] [(\Omega - 1/\Omega)/2i]. \tag{A.3}$$

By letting  $\Omega$  approach the unit circle at  $i e^{i\psi}$ , coordinates of the elastic-plastic boundary are

$$x_1 - ix_2 = -[K^2/2\pi\tau'(0)] (d\psi/d\tau) \cos \psi, \tag{A.4}$$

where  $d\tau/d\psi = i\Omega\tau'(\Omega)$ , and  $d\tau$  is directed along the yield surface. Note that  $d\psi = d\Phi$  and  $\cos \psi = \sin \Phi$ . When the yield surface contains flat segments,  $d\tau$  has a constant phase along them, and it is easy to verify that the segment maps into a straight-line plastic zone in the  $x_1, x_2$  plane, parallel to that segment, with  $x_1 = 0, x_2 = 0$  at the vertices terminating the segment. The radius to a given point is

$$R = [K^2/\pi\tau'(0)] |d\psi/d\tau| \cos \psi. \tag{A.5}$$

Displacements are discontinuous across these line plastic zones. Along them (RICE, 1984; equation (76))

$$u = R\tau_r/\mu - R_0\tau_{r0}/\mu + [K^2/\pi\mu\tau'(0)] (\sin \psi - \sin \psi_0), \tag{A.6}$$

where the subscript '0' refers to some value of  $\psi$  at which  $u = 0$ . The displacement discontinuity at the crack tip is (RICE, 1984; equation (77))

$$\Delta u = 2K^2/\pi\mu\tau'(0). \tag{A.7}$$

For the case of the yield surface of Fig. 4b, and with  $n$  defined as in Fig. 11a, we have by the Schwarz-Christoffel method that

$$\tau'(\Omega) = (\tau_0/\alpha) (1 - \Omega)^n / [(1 + \Omega)^n (1 - 2\Omega \cos \lambda + \Omega^2)^{(1+n)/2} (1 - 2\Omega \cos \omega + \Omega^2)^{(1-n)/2}], \tag{A.8}$$

where  $\alpha, \lambda$  and  $\omega$  are as yet undetermined. Writing  $\Omega = e^{i\Phi}$  on the boundary of the unit circle,

$$d\tau/d\Phi = (\tau_0/2\alpha) [\sin(\Phi/2)]^n / [\cos(\Phi/2)]^n [\cos \Phi - \cos \lambda]^{(1+n)/2} [\cos \Phi - \cos \omega]^{(1-n)/2}. \tag{A.9}$$

We need three conditions to determine  $\alpha$ ,  $\lambda$  and  $\omega$ . From Fig. 11 we see that points  $A, B, C$  and  $D$  lie on the unit circle in the  $\Omega$  plane and that corresponding points in the  $\tau$  plane lie on the yield surface, and that the following conditions must be satisfied

$$\overline{OA} = \overline{DO} = \overline{AB} = \tau_0 / \cos(n\pi/2). \tag{A.10}$$

These three conditions may be rewritten as

$$\alpha / \cos(n\pi/2) = F(\lambda, \omega) = G(\lambda, \omega) = H(\lambda, \omega), \tag{A.11}$$

where  $F, G$  and  $H$  are defined as

$$F(\lambda, \omega) = \int_0^1 [(1-x)^n / (1+x)^n (1-2x \cos \lambda + x^2)^{(1+n)/2} (1-2x \cos \omega + x^2)^{(1-n)/2}] dx, \tag{A.12}$$

$$G(\lambda, \omega) = \int_{-1}^0 \dots (\text{same integrand}) \dots dx,$$

$$H(\lambda, \omega) = \frac{1}{2} \int_0^\lambda [|\sin(\Phi/2)|^n / |\cos(\Phi/2)|^n |\cos \Phi - \cos \lambda|^{(1+n)/2} |\cos \Phi - \cos \omega|^{(1-n)/2}] d\Phi.$$

By use of numerical integration and iteration procedures the unknown parameters can be evaluated for the given value of the angle  $n\pi/2$ . For the case in Fig. 4a,  $n = 0.2163$ , and then we find  $\lambda = 0.5702$  rad =  $32.67^\circ$ ;  $\omega = 2.156$  rad =  $123.53^\circ$ , and  $\alpha = 0.9174$ . The radius along the line plastic zone is from (A.5 to A.9)

$$R = (2\alpha^2 K^2 / \pi \tau_0^2) [\sin \Phi |\cos(\Phi/2)|^n |\cos \Phi - \cos \lambda|^{(1+n)/2} |\cos \Phi - \cos \omega|^{(1-n)/2} / |\sin(\Phi/2)|^n]. \tag{A.13}$$

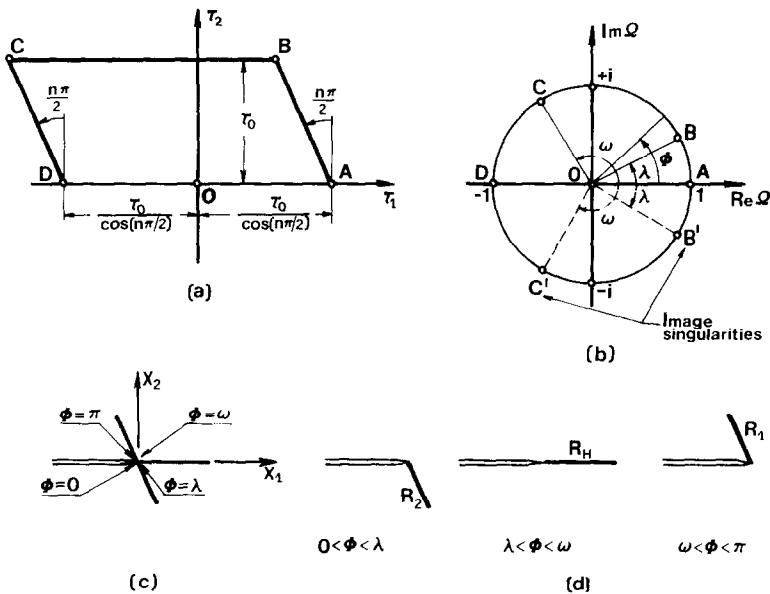


FIG. 11. (a) Yield surface in complex  $\tau$  plane; (b) unit circle in complex  $\Omega$  plane; (c) physical  $x_1, x_2$  plane; (d) discrete line plastic zones for different ranges of  $\Phi$ .

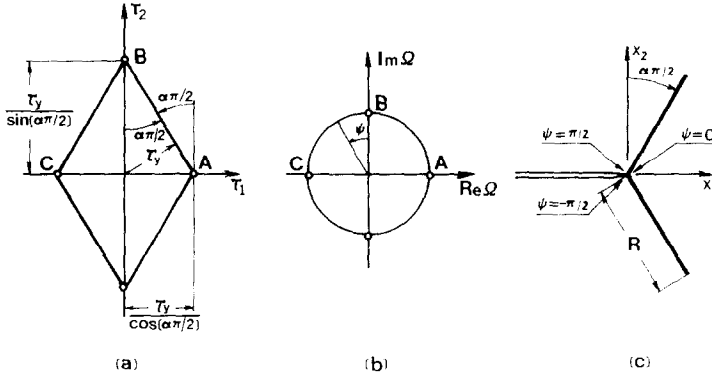


FIG. 12. (a) Yield surface in  $\tau$  plane; (b) unit circle in  $\Omega$  plane; (c) physical  $x_1, x_2$  plane.

and by maximizing this expression with respect to  $\Phi$  on the intervals  $0 < \Phi < \lambda$ ,  $\lambda < \Phi < \omega$ , and  $\omega < \Phi < \pi$  we obtain the plastic zone lengths quoted in the first subsection of section 4.

Next we consider the mapping of the yield surface for the three cases in the following subsections of section 4. All have shape of a diamond with vertices on the  $\tau_1, \tau_2$  axes; Fig. 12. Here  $\tau_y$  denotes the perpendicular distance of each straight-line segment from the origin of the  $\tau$  plane. Letting  $\alpha\pi/2$  be the angle indicated,

$$d\tau/d\Omega = M/(1 - \Omega^2)^2(1 + \Omega^2)^{(1-\alpha)}, \tag{A.14}$$

where  $M$  can be evaluated from either of the following equivalent expressions

$$\tau_y/\cos(\alpha\pi/2) = M \int_0^1 [1/(1-x^2)^\alpha(1+x^2)^{(1-\alpha)}] dx, \tag{A.15.1}$$

$$\tau_y/\sin(\alpha\pi/2) = M \int_0^1 [1/(1+y^2)^\alpha(1-y^2)^{(1-\alpha)}] dy. \tag{A.15.2}$$

Thus, the radius along a line plastic zone is

$$R = (2K^2/\pi M^2)(\sin \psi)^{(1-\alpha)}(\cos \psi)^{(1+\alpha)}. \tag{A.16}$$

Maximizing  $R$  on the interval for  $0 < \psi < \pi/2$  one obtains  $(dR/d\psi) = 0$  for  $\cos 2\psi - \alpha = 0$ , which gives the maximum plastic zone radius as

$$R = (2K^2/\pi M^2)[(1-\alpha)/2]^{(1-\alpha)/2}[(1+\alpha)/2]^{(1+\alpha)/2}. \tag{A.17}$$

Values of  $\alpha$  are 0.3918 in subsections two and four (section 4), and 0.5 for the third case in this section. The corresponding values of  $M$  are  $1.1080\tau_y$  ( $= 1.1080\tau_0$ ) for subsections two and four, and  $1.0787\tau_y$  ( $= 1.8684\tau_0$ ) for part three in section 4.